

Whole-Cell Patch-Clamp Recordings

Harald Sontheimer and Michelle L. Olsen

1. Introduction

The patch-clamp recording technique measures ionic currents under a voltage clamp and was designed to study small patches of membrane in which near-perfect control of the transmembrane voltage can be readily achieved. Today, this technique is most frequently used to examine currents across entire cells. This application defies many of the original design requirements, such as small size and near-perfect voltage control. Nevertheless, whole-cell recordings are routinely used to characterize current flow through ionic channels, neurotransmitter receptors, and electrogenic transporters in cell types of virtually any origin. Since its introduction in 1981 (Hamill et al., 1981), patch-clamp recordings have essentially replaced sharp electrode recordings, particularly in the study of cultured cells and more recently in brain slice recordings.

Whole-cell patch-clamp recordings and their applications have been the topic of numerous excellent reviews and book chapters (see Recommended Readings at the end of the chapter). This chapter summarizes some basic concepts and describes “hands-on” procedures and protocols, so as to complement previous accounts of the patch-clamp technique.

2. Principles (Why Voltage-Clamp?)

Electrophysiologists are especially interested in the activity of membrane proteins that provide conductive pathways through biological membranes: ion channels, transmitter receptors, and electrogenic ion carriers. Channel activity, whether through voltage-dependent or ligand-gated ion channels, results in changes of membrane conductance, which can be most conveniently evalu-

From: *Neuromethods*, Vol. 38: *Patch-Clamp Analysis: Advanced Techniques*, Second Edition
Edited by: W. Walz @ Humana Press Inc., Totowa, NJ

ated by recording membrane currents at a constant membrane voltage. Under such “voltage-clamped” conditions, current is directly proportional to the conductance of interest.

A two-electrode voltage-clamp design was first introduced in the seminal studies of Hodgkin and Huxley (Hodgkin et al., 1952) for the study of ionic conductances of the squid giant axon. In this application, one of the electrodes serves as voltage sensor and the second functions as a current source, with both interconnected through a feedback amplifier. Any change in voltage detected at the voltage electrode results in current injection of the proper polarity and magnitude to maintain the voltage signal at a constant level. The resulting current flow through the current electrode can be assumed to flow exclusively across the cell membrane and as such is proportional to the membrane conductance (mediated by plasma membrane ion channels). The major disadvantage of this technique, however, is its requirement for double impalement of the cell, which restricts its application to rather large cells ($>20\mu\text{m}$) and prevents study of cells embedded in tissue.

In an attempt to solve this problem, single-electrode switching amplifiers were developed that allowed the use of one electrode to serve double duty as voltage and current electrode. For short periods of time, the amplifier connects its voltage-sensing input to the electrode, takes a reading, and subsequently connects the current source output to the same electrode to deliver current to the cell. This approach, however, is limited in its time resolution by the switching frequency between the two modes, which must be set based on the cell's RC time constant (the product of cell input resistance R and capacitance C). Both single-electrode switch clamp and double-electrode voltage clamp allow direct measurement of the cell's voltage and avoid the introduction of unknown or unstable voltage drops across the series resistance of the current passing electrode.

The whole-cell patch-clamp technique similarly uses only one electrode. However, in contrast with above techniques, it uses the electrode continuously for voltage recording and passage of current. Consequently, the recording arrangement contains an unknown and potentially varying series resistance in the form of the electrode and its access to the cell. For the technique to deliver satisfactory results, it is essential that this series resistance be small relative to the resistance of the cell. Numerous measures are taken to satisfy these requirements (see below), including the use of blunt, low-

resistance electrodes, small cells with high impedance, and electronic compensation for the series resistance error. When effectively utilized, the whole-cell technique can yield current recordings of equal or superior quality to those obtained with double- or single-electrode voltage-clamp recordings.

3. Procedure and Techniques

3.1. Pipettes

In contrast with sharp electrode recordings that utilize pipettes with resistances of $>50\text{ M}\Omega$, comparatively blunt low-resistance ($1\text{--}5\text{ M}\Omega$) recording pipettes are used for whole-cell patch-clamp recordings. This is done for two reasons: (1) series resistance should ideally be two orders of magnitude below the cell's resistance, and (2) blunt electrodes ($1\text{--}2\text{ }\mu\text{m}$) are required to achieve and maintain mechanically stable electrode-membrane seals.

As described in Chapter 1, electrodes can be manufactured from a variety of glass types. Although it has been frequently reported that glass selection has a significant influence on the quality of seal or the frequency at which good seals are obtained, little scientific evidence supports this notion. To achieve the shape ideal for sealing membrane patches, electrodes are pulled from capillary glass pipettes in a two-stage or multistage process using commercially available pullers, such as those of Narashige (Tokyo, Japan), Sutter (Novato, CA), and others. An additional step of fire-polishing the pipette tip may be used to improve the likelihood of seal formation. As an added benefit, the tips of pipettes with very low resistance (steep, tapering tips) can be fire-polished to reduce the tip diameter to appropriate levels. Once an appropriate set of variables, such as cell preparation, glass type, electrode resistance, and shape, is identified, the success rate for stable electrode-membrane seals should be between 50% and 90%.

3.2. Electronic Components of a Setup

The electronic components of a patch-clamp setup are comparatively few: a patch-clamp amplifier, a digital-analog/analog-digital converter, and a computer. An oscilloscope, external stimulator, or external signal filters, and recording devices are options. High-quality patch-clamp amplifiers are available from a number of

manufacturers. At present, many laboratories utilize either a Heka EPC 9/10 (Southboro, MA), or an Axopatch 200B, or MultiClamp 700B amplifier (Molecular Devices, Sunnyvale, CA). Most manufacturers design their amplifiers to offer a broad range of functions (whole-cell recording, single-channel recording, current clamp, voltage clamp). However, some amplifiers are particularly tailored for specific functions, such as recording from lipid bilayers. Caution must be exercised, especially by the novice electrophysiologist, in using computer-controlled amplifiers such as the Axopatch 700B. Many features including pipette offset, series resistance, compensation, and whole-cell capacitance, which on traditional amplifiers must be adjusted manually, are automatically determined by the amplifier, communicated to the software, and stored. Previous experience on traditional amplifiers provides the users of automated amplifiers with the experience to determine the reliability and validity of these values.

The single most important electronic component of a patch-clamp amplifier is the current-to-voltage converter, which is contained in the head stage (Fig. 1). Its characteristics are described in detail elsewhere (Sigworth, 1983). Until recently, most head stages used resistive technology. Here current flow through the electrode (I_p) across a resistor of high impedance (R) causes a voltage drop that is proportional to the measured pipette current (I_p). An operational amplifier (OpAmp) is used to automatically adjust the voltage source (V_s) to maintain a constant pipette potential (V_p) at the desired reference potential (V_{ref}). As the response of the OpAmp is fast, it can be assumed that for all practical purposes $V_p = V_{ref}$. When

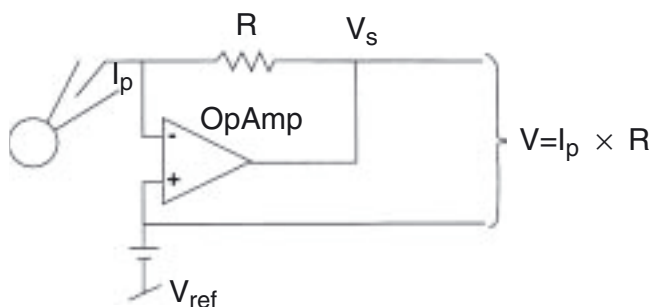


Fig. 1. Scheme of current-to-voltage converter (for details see Sigworth, 1983). I_p , pipette current; R , feedback resistance; OpAmp, operational amplifier; V_{ref} , reference potential; V_s , voltage source.

current flows across the membrane through ion channels, V_p is instantaneously displaced from V_{ref} . The OpAmp alters V_s to generate an I_p that will exactly oppose the displacement of V_p from V_{ref} . Thus, the current measured during a patch-clamp experiment (membrane current flow) is equal and opposite to I_p .

In their whole-cell mode, resistive patch-clamp amplifiers use a 500 M Ω feedback resistor, which enables measuring currents of up to 20 nA. For some amplifiers a low-gain 50 M Ω head stage is available that can pass currents of up to 200 nA; however, its use sacrifices the use of capacitance and series resistance compensation. More recently, amplifiers such as the Axopatch 200B or 3900A Integrating Patch Clamp (Dagan, Minneapolis, MN) have head stages that operate in two modes: traditional resistive feedback for whole-cell recording, and capacitor feedback or integrating mode for single-channel recording. Because capacitors generate less noise than resistors (an ideal capacitor generates no thermal noise), the instrument or circuit noise associated with the resistor is eliminated when recording in integrating mode, allowing for extremely low noise during single-channel recording.

Although some amplifiers, such as the Axopatch 1D, have built-in stimulators, most electrophysiologists prefer the use of an external stimulator that offers greater versatility. Low-cost microcomputers serve as both digital stimulator and on-line recorder. While the use of a microcomputer is not essential, it has become the de facto norm, as the convenience of storing and analyzing digital data far outweighs the cost associated with such systems. Moreover, most systems are now highly integrated, such that the amplifiers communicate via telegraphs many important analog settings such as gain, capacitance, series resistance, and filter frequency settings. In addition they provide for easy delivery of stimulus protocols via their digital/analog (D/A) converters. Data can be collected and digitized on-line with sampling rates of up to 5 μ s and can be readily stored on the hard disk of a computer. All necessary components can be purchased at a price well below that of an external stimulator alone.

Additional equipment is recommended for specific data collection needs, and it is not uncommon to find an oscilloscope or even a VCR recorder attached to a recording setup. The latter, however, has become unpopular with the introduction of relatively inexpensive large hard drives and convenient inexpensive means to back up data digitally on CDs and DVDs. Even in the presence of a

computer-based data acquisition system, oscilloscopes are a convenient means for monitoring data collected by a microcomputer, and are convenient for debugging environmental electrical noise from a recording setup. If nothing else it conveys the “cockpit look” to a patch-clamp setup and provides enough counterweight to the equipment rack to prevent it from tipping over.

3.3. Recording Configuration

The whole-cell patch-clamp recording setup closely resembles that used for sharp electrode intracellular recordings. An electrically grounded microscope on an isolation table serves as the foundation of the recording setup. A recording chamber is mounted to the stage of an inverted microscope for isolated cell recording (Fig. 2A) or an upright microscope with a water immersion lens for slice recording (Fig. 2B). Various types of recording chambers are commercially available, all of which serve well for most purposes. If perfusion is desired, several options are available, including constant perfusion via peristaltic pump, gravity-fed perfusion systems, and systems that allow for an ultrafast fluid exchange. Electrodes are typically placed under visual control (400×) onto a cell by use of a high-quality, low-drift micromanipulator.

Numerous hydraulic, piezoelectric, motorized, and mechanical designs are commercially available, each offering unique benefits. Motorized manipulators, such as Sutter model MP-225 (Novato, CA), combine precise movement with large travel, and are very versatile and easy to use (Fig. 2B). These types of manipulators usually have different settings, which allow for both fine and coarse movement in the x, y, and z planes. Piezoelectric manipulators, such as the Burleigh PCS 5000 (McHenry, IL), allow only 150 μm of piezoelectric travel, and as such are useful only in combination with a coarse positioning manipulator. Piezoelectric systems provide excellent stability and are the instruments of choice for excising patches for single-channel recordings. Stable, low-cost mechanical manipulators (such as Soma Instruments series 421, Irvine, CA) can be assembled from single-axis translation stages. The arrangement shown in Fig. 2A includes three 421 stages of which the x and y axes are controlled manually by micrometer screws, whereas the z axis for electrode placement on the cell uses an 860 DC motor controlled by a hand-held battery-operated manipulator (model 861). Their modular design, combined with

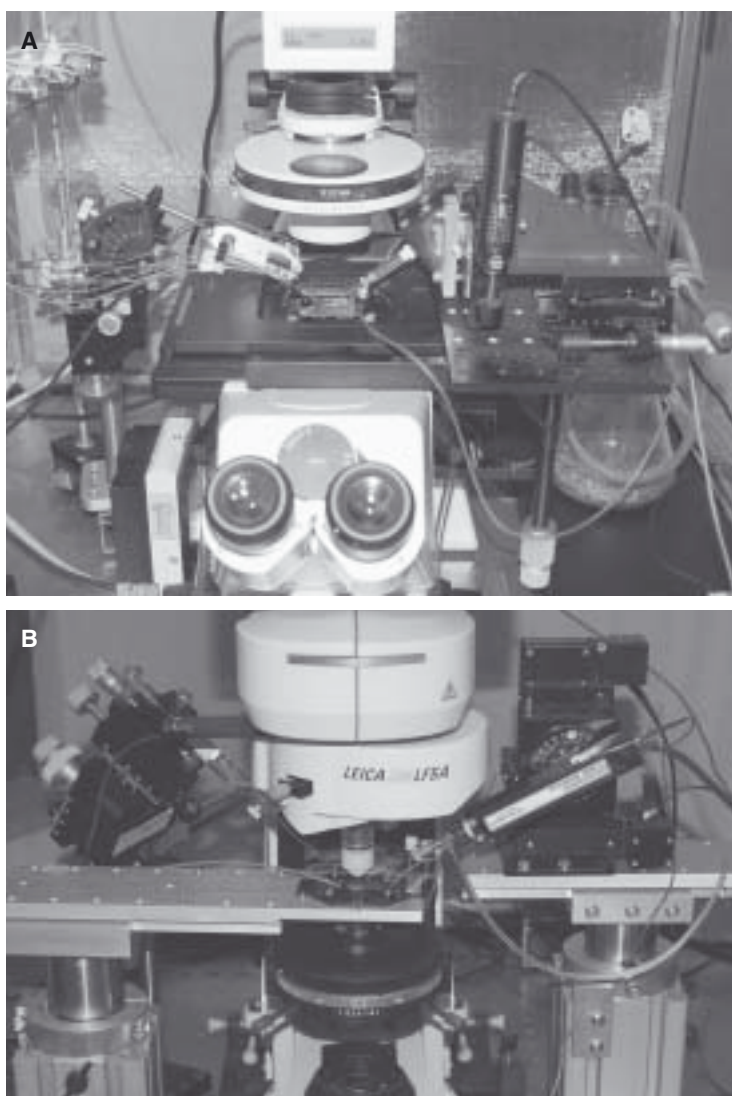


Fig. 2. Whole-cell cultured patch clamp setup (A) and slice recording setup (B). Photomicrographs of a typical recording setup based on a Zeiss Axiovert inverted microscope with a movable stage. Patch-clamp head stage with electrode holder mounted on a swivel clamp and attached to a three-axis manipulator constructed from three series 420 microtranslation stages (Newport Corporation, Irvine, CA). (B) Leica DMLFSA (model type) upright microscope with a fixed stage and water immersion lens for slice recording. Patch-clamp head stage mounted to a motorized manipulator (Sutter model MP-225).

micrometer screws and DC motors (e.g., model 860A) make them extremely versatile (Fig. 2A).

3.4. Experimental Procedure

During electrode placement, electrode resistance is monitored continuously by applying a small voltage pulse (1–5 mV, 2–10 ms) to the electrode (Fig. 3A). Once contact is made with the cell, electrode resistance spontaneously increases by 10% to 50%. Application of gentle suction to the electrode by mouth or a small syringe quickly results in the formation of a gigaseal (Fig. 3B). At this point, seal quality can be improved by applying a negative holding poten-

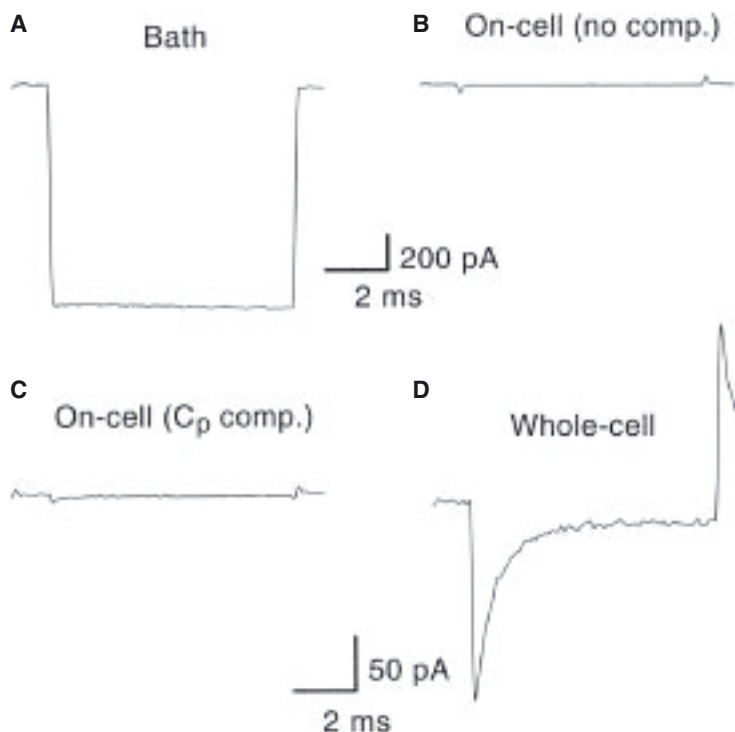


Fig. 3. Oscilloscope traces before and during establishment of whole-cell recording. (A) Electrode in bath ($V = 0$ mV). (B) On cell after formation of gigaseal ($V = 0$ mV). (C) As in B, after C_p compensation (comp.). (D) After rupturing patch, whole-cell configuration but prior to cell capacitance and series resistance compensation ($V = -80$ mV).

tial to the pipette. In this cell-attached configuration, pipette capacitance transients (C_p) are reduced using the fast compensation adjustment at the amplifier (Fig. 3C). Compensation of pipette capacitance is essential for subsequent series resistance compensation. Should compensation be incomplete, coating of future electrodes with Sylgard (Dow Corning, Midland, MI) or lowering the bath perfusion level is recommended to reduce the residual transients and improve C_p compensation.

Following pipette capacitance cancellation, a brief pulse of suction will rupture the membrane patch under the electrode, providing low-resistance access to the cell. This also results in a large-capacity transient arising from the added membrane capacitance (Fig. 3D). Immediately after rupturing the membrane, a reading of the cell's potential should be obtained (at $I = 0$), as this access potential is as close to the actual resting potential reading that can be obtained. Within minutes of establishing a whole-cell configuration, the pipette contents will equilibrate with the cell's cytoplasm and will impose an artificial ionic potential across the membrane. Next, by adjusting the capacitance and series resistance (R_s) compensation and gradually increasing the percent of compensation, effective R_s compensation should be possible under most circumstances. Ideally, access resistance should be $<10\text{ M}\Omega$ prior to activating R_s compensation. Under these conditions 80% compensation results in a $<2\text{ M}\Omega$ residual uncompensated series resistance. Series resistance and capacitance compensation result in a change of the step waveform applied without actually changing access resistance or the cell capacitance per se (see below). The procedure for establishing whole-cell configuration and all necessary compensations are nicely illustrated in the manuals from most amplifiers.

Due to the intracellular perfusion of cytoplasm with pipette solution, it is advisable to wait several minutes prior to obtaining recordings to assure that this dialysis has reached a steady state. Diffusion rates depend on the molecular weight and the charge of the diffusing particle, such that longer diffusion times are expected for relatively large, uncharged molecules as compared to small ions. For substances of molecular weight 23,000 to 156,000, diffusion rates have been determined in adrenal chromatin cells, and these rates suggest that complete dialysis of these small cells occurs on the order of tens to hundreds of seconds (Pusch and Neher, 1988). If dialysis of the cell is incompatible with the experimental

design, for example, when ionic currents are studied, which are under control of second messengers, the perforated-patch method should be used instead.

4. Data Evaluation and Analysis

4.1. Data Filtering/Conditioning, Acquisition, and Storage

4.1.1. Filtering

Data are hardly ever acquired and stored without further modifications. The analog output of the amplifier is typically amplified to make effective use of the dynamic range of the acquisition device. In the case of an A/D converter, this typically translates to an amplification range of -10 to 10 V. At the same time, signals are filtered, often using the built-in signal filter. Filtering of data is both essential and inevitable. Due to the RC components of the cell membrane–series resistance combination, the cell and electrode are essentially a single-stage RC filter. This is important to bear in mind, as it can significantly affect the true time-resolution of a recording. Assuming that $R_s \ll$ membrane resistance (R_m), uncompensated R_s will filter any current flow recorded with a -3 dB cutoff frequency described by $F = 1/(2\pi * R_s * C_m)$. Assuming, for example, a cell capacitance of 20 pF and a series resistance R_s of 10 M Ω (values typical of small cell recordings), currents across the membrane will be filtered with an effective F of ~ 800 Hz.

Irrespective of the intrinsic filter properties of the analyzed cell, data filtering is essential to reduce signal components that are outside the bandwidth of interest. Filtering condenses the time domain of the signal to the domain of interest. The fastest signals recorded under whole-cell conditions are on the order of 200 to 500 μ s (2 – 5 kHz). Note that this is of the same order of magnitude as the membrane- R_s filter time-constant above. To eliminate high-frequency noise, a low-pass filter is used. An ideal filter has a steep roll-off, and does not greatly distort signals. A four- or eight-pole Bessel filter has excellent characteristics for filtering whole-cell currents. The filter characteristics of a four- and eight-pole Bessel filter are demonstrated by comparing the onset response of a square pulse before and after filtering at various cutoff frequencies (Fig. 4). In these examples, an eight-pole Bessel filter clearly provides excellent signal filtering with the least distortions. However, at cutoff frequencies above 2 kHz, the four- and eight-pole filters do not differ significantly in the onset or settling time.

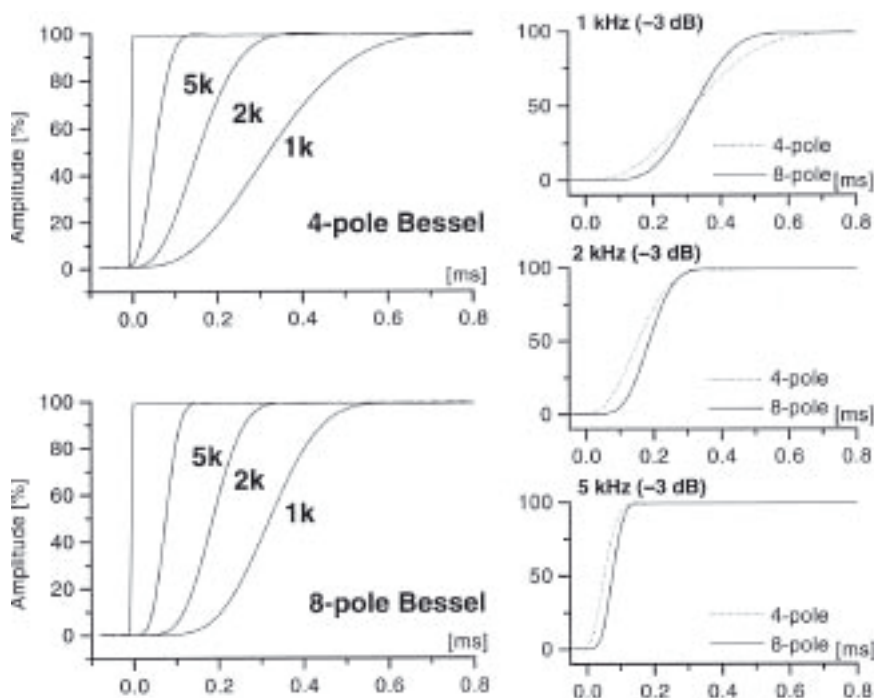


Fig. 4. Frequency response of a four- and eight-pole Bessel filter to square pulse. A 2-ms square pulse was applied to a frequency device model 902 eight-pole Bessel filter as compared to the built-in four-pole Bessel filter of the Axopatch 1D amplifier. The graphs illustrate differences in response characteristics at 3 commonly used 3-dB cutoff frequencies (1, 2, and 5 kHz).

4.1.2. Sampling Rate and Dynamic Range of Signal

When using an A/D converter to digitize signals, it is important to select the appropriate filter and sampling rates to accurately represent the analog signal of interest. It is inevitable that A/D conversion will reduce the infinite dynamic range of the analog signal to a well-defined step-like range of the digital signal. Commonly used 12-bit converters (for example, the Axon Digidata 1200, Molecular Devices, Sunnyvale, CA) divide the amplitude range into 4,096 discrete steps, which at a -10 to 10 V signal range will yield steps of 4.88 mV. In theory, signals can be sampled at the highest possible rate supported by the A/D converter. However, practical limitations exist. Most affordable A/D boards sample at

100 to 330 KHz on a single channel, thus allowing sampling in 3- to 10- μ s intervals. Depending on the duration of the signal, sustained sampling at 10 μ s generates very large amounts of data, requiring significant disk space. A vast majority of these data do not contain necessary information.

The Nyquist sampling theorem states that the minimum sampling rate (Nyquist frequency) required to accurately represent an analog waveform is twice the signal bandwidth. As a consequence, if the analog filter is set at a -3 dB cutoff frequency of 3 kHz, a minimum sampling frequency of 6 kHz or 167- μ s intervals is required. While these minimum requirements allow the reconstruction of data with little error under most circumstances, a sampling frequency five times the -3 dB frequency is commonly recommended for actual recordings.

4.1.3. Aliasing

The Nyquist sampling theorem only applies when sampling data digitally at frequencies between 0 and the Nyquist frequency. If frequencies higher than the Nyquist frequency are sampled, they are "folded back" into the low-frequency domain, a process called aliasing. Essentially these high-frequency signals affect and distort those signals within the appropriate frequency domain. Aliasing can be prevented if signals above the Nyquist frequency are cut off by a low-pass filter. A proper matching of filter frequency and sampling rate is thus important to accurately reproduce analog waveforms. In practical terms this requires that the cutoff frequency of a low-pass filter be set to no higher than half the sampling frequency. In the example above, the low-pass filter was set at 3 kHz.

4.1.4. Data Storage

On-line digitization has the advantage that data can be directly stored in computer memory or on a hard drive. This mode of data storage is preferred, as it gives convenient and fast access to the data for future evaluation. Using a 12-bit A/D converter, each data sample uses 2 bytes of information. Thus a 2,048 sample trace requires about 4 kbytes of memory or disk space. A continuous sampling of neuronal discharge at a frequency of 50 kHz generates 100 kbytes of data every second. A 5-minute recording would thus require 300*100 kbytes or 30 Mbytes of disk space. It thus becomes apparent that practical limitations exist for on-line digitization of

data. For prolonged recordings at high frequencies, a VCR recorder (such as the Neurocorder digitizing unit, Pasadena, CA) may be used as an interim storage for data. Segments can subsequently be played back to the A/D converter for data analysis. However, this approach is less popular now that disk space has become so inexpensive. Recordable CD-R disks are a practical and inexpensive way to archive data.

4.2. Leak/Subtraction

Currents across a cell membrane consist of two components: ionic current flowing through ion channels of interest, and capacitive current that charges the membrane. Capacitive current contains useful information pertaining to the cell size, as an approximation of cell size (or more precisely, membrane area of the recorded cell) can be derived from the capacitive current. However, in the study of ionic currents, capacitive currents are of relatively little interest. As ideally capacitive currents are linear and not voltage dependent, they can be subtracted from the signal of interest through a process called leak subtraction. This subtraction can be done either on-line or off-line.

Two protocols for leak subtraction are typically used: (1) If the nature of the experiments permits, currents are recorded sequentially in the absence and presence of specific ion channel blockers [e.g., tetraethylammonium (TEA), tetrodotoxin (TTX), and 4-aminopyridine (4-AP)]. As specific blockers eliminate ionic current but should not alter the capacitive or leakage current, subtraction of the two traces or set of traces should result in the removal of capacitive and leakage currents. (2) If the first protocol cannot be used, P/N leak subtraction as first proposed by Bezanilla and Armstrong (1977) can be done. In this subtraction scheme, each test voltage step is preceded by a series of N (typically 4) leak voltage steps of $1/N$ ($1/4$ or $-1/4$, dependent on polarity) amplitude of the test pulse activated from a potential at which no voltage-activated currents are activated. In a $P/4$ protocol, these $4 \times 1/4$ amplitude traces are summed together (Fig. 5B) and are subtracted from the actual current trace of interest (Fig. 5A) and isolate the ionic current of interest (Fig. 5C).

The example demonstrated in Fig. 5 actually used a $P/-4$ protocol, in which four hyperpolarizing pulses of $-1/4$ amplitude were summed and added to the current trace of interest. It is important to obtain the leakage current at potentials at which no voltage-activated currents occur. Most often this can be achieved by stepping

to potentials negative of the resting potential (as illustrated). However, some cells express inwardly rectifying (or anomalous rectifying) currents that are active at the resting potential and negative thereof. Under these circumstances leak currents must be recorded at potentials at which the I - V curve is linear and no voltage-dependent currents are activated. Note that subtraction of capacitive and leakage currents is purely cosmetic. It does not actually improve the signal recorded. However, it may reveal small current components that would otherwise be difficult to identify.

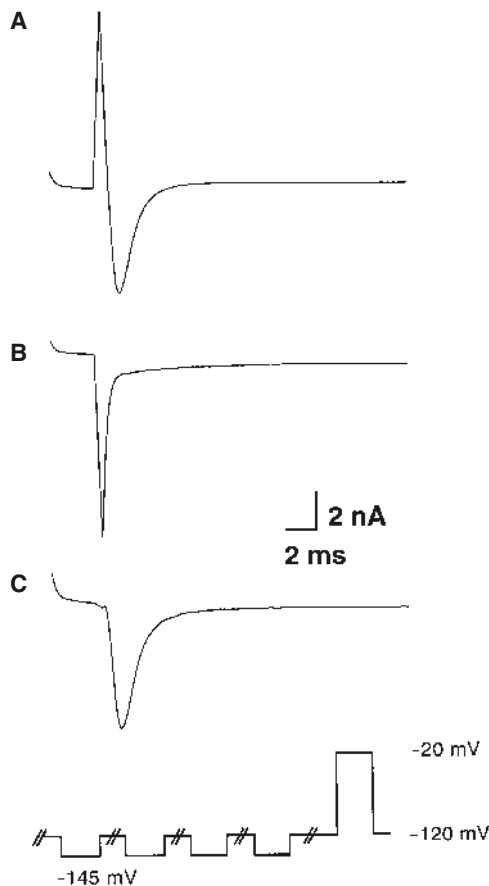


Fig. 5. Capacitive and leakage current subtraction using $P/-4$ method. (A) Whole-cell current recorded in response to voltage step from -120 mV to -20 mV. (B) Summed response of $4 \times 1/4$ amplitude voltage steps as indicated at bottom of C. (C) Added response of A and B eliminating capacitive current.

If capacitive currents are not of interest, it is recommended that $P/4$ leak subtraction be performed on-line by the data acquisition program since it significantly reduces the amount of data stored.

4.3. Determination of Cell Capacitance

Biological membranes are lipid bilayers in which membrane proteins (e.g., ion channels and transporters) are contained. The specific capacitance of biological membranes seems to be fairly constant. It is relatively independent of cell type, and a value of $1\mu\text{F}/\text{cm}^2$ is typical. The capacitance cancellation circuits of patch-clamp amplifiers are normally calibrated in picofarads (pF), and allow direct determination of the cells' capacitance by adjusting and minimizing the capacity transients in response to a voltage step as discussed previously. The dial reading provides at least a rough determination of membrane capacitance on the basis of which estimates can be made as to the membrane area, as 1pF capacitance represents $100\mu\text{m}^2$ of membrane.

Capacitance can also be derived from the capacity transient at any time during the recording. In response to a voltage step, capacitance is proportional to the integral of the charging transient; thus, it can be derived by determining the area under the transient of a current's trace. Neher and Marty (1982) have developed a very sensitive approach to measuring changes in membrane capacitance using a phase-lock amplifier, which measures currents in and out of phase with a sinusoidal voltage change. This approach can resolve capacitance changes of 10 femto seimens (fS) and has been used to resolve the fusion of synaptic vesicles by a step increase in capacitance.

4.4. Dissecting Current Components

Whole-cell recordings integrate the response of a large number of potentially heterogeneous ion channels. Separation of these ionic current components is a critical step during or following current recordings. Four methods of current isolation are commonly used to isolate voltage-activated ionic currents:

4.4.1. Kinetic

Certain types of ion channels activate and inactivate much faster than others. For example, Na^+ currents typically activate within 200 to $300\mu\text{s}$ and inactivate completely within 2 to 5 ms. In contrast, K^+

currents may take several milliseconds to activate, and often inactivate slowly, if at all. Simple current isolation can thus be accomplished by studying whole-cell currents at different time points following stimulation, for example, determining Na^+ current amplitudes at 300 to 500 μs , and determining K^+ current amplitudes after tens or hundreds of milliseconds.

4.4.2. Current Subtraction via Stimulus Protocols

Voltage-dependence of the steady-state activation and inactivation of currents often allows selective activation of subpopulations of ion channels. For example, low- or high-threshold Ca^{2+} currents can be activated separately by voltage steps originating from different holding potentials. Similarly, depolarizing voltage steps applied from very negative holding potentials (e.g., -110 mV) can activate both transient A-type (K_A) and delayed-rectifying (K_d) K^+ currents (Fig. 6A). Voltage steps applied from a more positive holding potential (e.g., -50 mV) completely inactivate all K_A channels while not affecting K_d activity (Fig. 6B), such that subtraction of currents recorded with these two protocols effectively isolates K_A currents (Fig. 6C).

4.4.3. Isolation Solutions (Ion Dependence)

It is common practice to specifically design the composition of ionic solutions to favor movements of desired ions. As mentioned previously, dialysis of cytoplasm with patch pipette contents occurs rapidly after whole-cell configuration is achieved, thus allowing for manipulation of internal ionic concentrations. This access can be used to block most K^+ channel activity by replacing pipette KCl with impermeant Cs^+ or *N*-methyl-D-glucamine (NMDG), thus allowing isolation of Na^+ currents. In a similar fashion, acetate, gluconate, or isothionate can each be substituted for Cl^- ions, and tetramethyl-ammonium chloride (TMA-Cl) can be substituted for Na^+ ions. It has even been reported that the contribution of one ion channel population can be determined by replacement of all but the desired ion with glucose or sucrose.

4.4.4. Current Isolation via Pharmacology

Numerous natural toxins and synthetic pharmacological agents can be used to reduce or eliminate specific voltage-activated ion channel activity. Table 1 lists some of the more commonly used

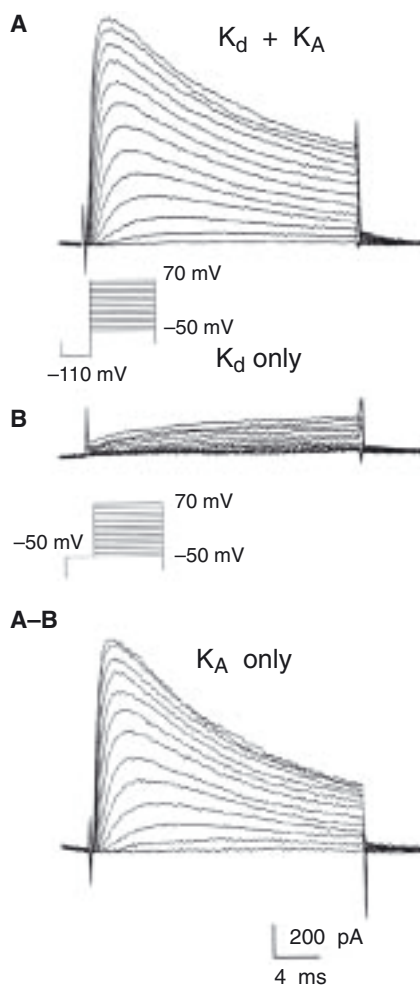


Fig. 6. Isolation of K_A current by subtraction. Current recordings from a spinal cord astrocyte expressing both transient (K_A) and delayed rectifier (K_d) like K^+ currents. (A) Currents activated from holding potential of -110 mV. (B) Same cell and same voltage step protocol, but steps originated from holding potential of -50 mV. Subtraction of A-B yielded K_A currents in isolation.

agents, many of which are effective against one particular type of ion channel, such as tetrodotoxin and dendrotoxin, which target Na^+ and K^+ channels, respectively. The use of these compounds, either alone or in combination, allows the isolation of specific current(s).

Table 1
Commonly used ion channel blockers

Channel type	Compound/reagent
<i>K⁺ channels</i>	
Delayed rectifier (K_d)	TEA, Ba^{2+} , capsaicin, 4-AP, margatoxin, 9-AC, charybdotoxin
Inward rectifier (K_{ir})	TEA, Cs^+ , Rb^+ , Na^+ , Ba^{2+} , tertiapin,
Gaboon viper venom, LY-97241	
Fast inactivating (K_A)	TEA, 4-AP, dendrotoxin, quinidine
$K(Ca)$	
BK	Charybdotoxin, iberiotoxin, paxilline, TEA
SK	Apamin
IK	Clotrimazole, cetiedil
K(ATP)	TEA, Cs^+ , Ba^{2+}
<i>Na⁺ channels</i>	TTX, STX, CNQX, agatoxin, scorpion toxin
<i>Ca²⁺ channels</i>	
L-type	Nifedipine, verapamil, BayK8644,
Cd^{2+} , La^{3+} , nimodipine, ω -agatoxin IIIA	
T-type	Ni^{2+} , La^{3+} , mibefradil
N-type	ω -conotoxin, La^{3+}
P-type	FTX funnel spider toxin, ω -agatoxin IVA
<i>Cl⁻/anion channels</i>	Chlorotoxin, NPPB, DIDS, niflumic acid
	SITS, 9-AC, mibefradil, Cd^{2+} , Zn^{2+}

TEA, tetraethylammonium; 4-AP, 4-aminopyridine; 9-AC, 9-aminocamptothecin; TTX, tetrodotoxin; STX, saxitoxin; CNQX, 6-cyano-7-nitroquinoxaline-2,3-dione; NPPB, 5-nitro-2-(3-phenylpropylamino) benzoic acid; DIDS, 4,4'-diisothiocyanatostillbene-2,2'-disulfonic acid; SITS, 4-acetamido-4'-isothiocyanatostillbene-2,2'-disulfonic acid.

Experimentally, currents are best identified pharmacologically by recording a family of current traces in both the absence and presence of the drug. This is illustrated in Fig. 7, in which the block of spinal cord astrocyte K^+ currents by 4-AP is shown. In the control and treated current traces (Fig. 7A,B), the inward sodium current is unaltered. By subtracting the 4-AP-treated current traces from those of control, one can isolate the current component that is 4-AP-sensitive. As discussed previously, a side benefit to such current subtraction is the elimination of capacitive and leakage currents.

Neurotransmitter-activated currents are perhaps easier to identify and isolate than their voltage-dependent counterparts, as these currents are induced in a time-dependent manner based on the application of exogenous ligands. If need be, ligand-gated current

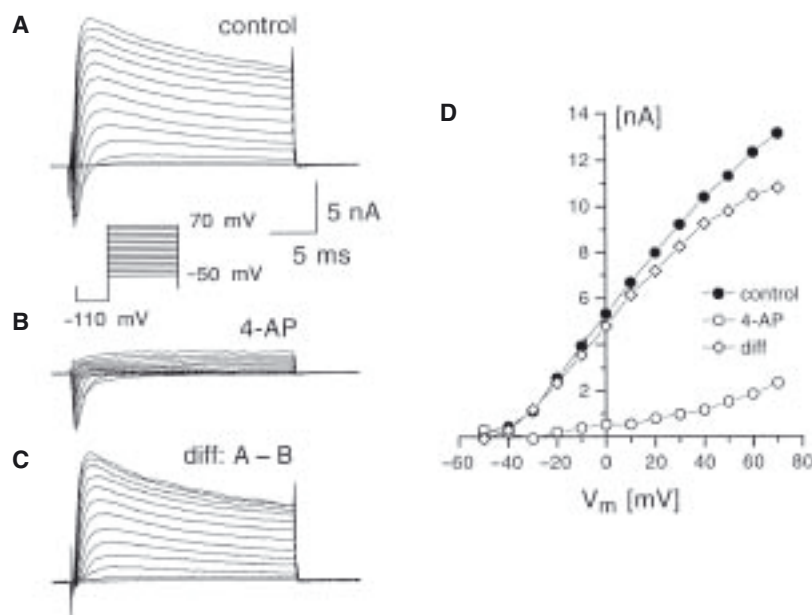


Fig. 7. Pharmacological isolation of 4-amino pyridine (4-AP)-sensitive K^+ current. (A) Family of current traces recorded from a spinal cord astrocyte. (B) Recording in the same cell using the same stimulus protocol 2 minutes after application of 2 mM 4-AP. (C) 4-AP-sensitive current isolated by subtraction of A-B. (D) Current amplitudes determined 8 ms after onset of voltage steps plotted as a function of applied potential for current traces in A-C.

can be isolated from background noise by subtracting recorded currents in the absence and presence of a given ligand.

4.5. I-V Curves

Current-voltage (I - V) relationships are perhaps the most effective way to summarize the behavior of voltage- and ligand-activated ion channels. A number of important and useful parameters that cannot be easily accessed from the raw data can be readily derived from these plots, including reversal potential, ionic dependence/selectivity, voltage-dependence (rectification), activation threshold, slope and cord conductance, as well as overall quality of voltage-clamp. The I - V curves can be determined in various ways, examples of which are discussed below.

The factors that determine current flow through an open channel are conductance and driving force. While conductance is proportional to the number of open channels, driving force is defined as the difference between actual voltage and the equilibrium potential for the ion(s) permeating the channel, also known as reversal potential (V_{rev}). Thus current can be described as $I = G (V_m - V_{\text{rev}})$.

A plot of I versus V_m is commonly used to derive G (slope) or V_{rev} (x-intercept). The current evoked at a given V_m can be measured using a variety of protocols, as discussed in the following subsections.

4.5.1. Peak and Steady-State I - V Curves

Peak currents are measured as the largest current activated by the applied voltage (Fig. 7C). Thus, if a current has a transient peak current amplitude, such as the K_A current in Fig. 7A, analysis software can easily determine maximal current and plot these values against voltage (Fig. 7C). If the current to be studied does not have this defined peak, steady-state values may be used, typically as recorded at the end of a voltage step. This type of analysis was applied to the 4-AP-treated current traces of Fig. 7B, with the resulting amplitudes similarly plotted in Fig. 7C.

4.5.2. Continuous Quasi-Steady-State I - V Curve

A convenient way to establish I - V curves is by alteration of the membrane potential in a continuous way through a voltage ramp. As this ramp can be applied very slowly, it permits the acquisition of a quasi-steady-state I - V relationship. This procedure has proven very useful in determining I - V relationships for transmitter responses. Note, however, that this approach assumes that currents do not inactivate during the length of the voltage ramp. An example of a voltage ramp used to determine the reversal potential of γ -aminobutyric acid (GABA)-induced currents is illustrated in Fig. 8. Here, a 200-mV, 400-ms voltage ramp (as indicated in the inset to Fig. 8A) was applied twice—once prior to application of GABA (control) and once during transmitter application (GABA). By subtracting the two responses, one obtains the transmitter-induced current in isolation. As the time axis represents a constant change in the voltage applied, it can be instantaneously replotted as an I - V relationship of the transmitter-induced current (Fig. 8B). Using this approach, I - V curves of transmitter responses can be easily created

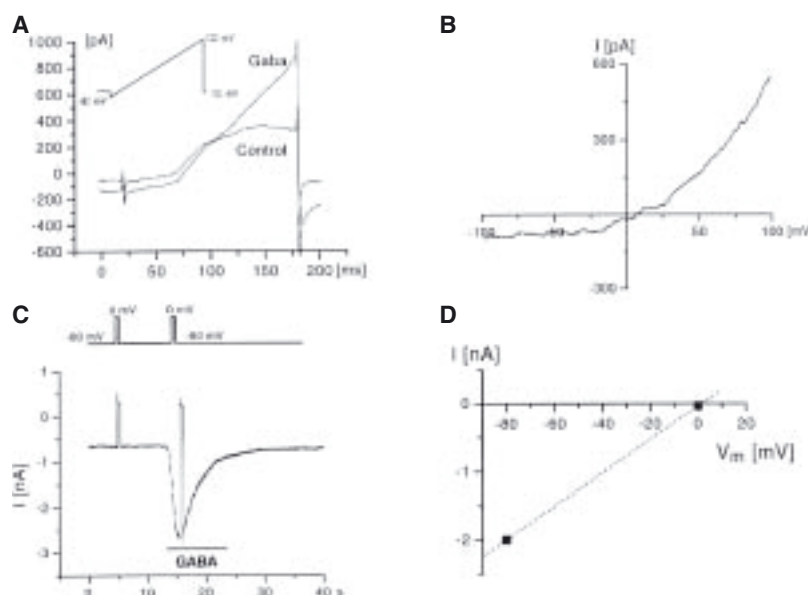


Fig. 8. Stimulus protocols to define reversal potential of γ -aminobutyric acid (GABA)-induced currents. (A) A voltage ramp (inset) was applied prior to (Control) and at the peak of GABA-induced currents. The difference of these two current ramps represent the GABA-induced current in isolation. (B) This current was plotted as a function of applied potential to yield the I - V curve of GABA-induced currents. (C) A single 50-ms, 80-mV voltage step was applied once prior to and once in the peak of the GABA response. (D) The differences of current amplitudes were plotted as a function of applied potential to yield two points of an I - V curve for GABA-induced currents. The dotted line extrapolates the current reversal potential.

throughout an experiment. As mentioned above, alteration of ionic composition shifts the reversal potential and thus allows determination of ion specificity and relative permeabilities.

For those situations where currents inactivate rapidly, some indication as to the reversal potential can be obtained using a single-step protocol from which the reversal potential can be extrapolated. An example of this approach is illustrated in Fig. 8C. Here, a larger concentration of GABA was bath applied, which resulted in characteristic receptor desensitization. The cell was maintained at -80 mV and a single 80-mV step (50 ms) was applied prior to and at the peak of the transmitter response. Current levels at the two

potentials, -80 mV and 0 mV , were then subtracted and plotted as a function of the applied potential (Fig. 8D). The line through the two data points clearly does not reflect the true I - V relationship of the response; however, it facilitates determining with fair accuracy the reversal potential of the response. To obtain a more complete I - V relationship, the two voltage steps above can be substituted by trains of voltage steps.

The I - V plots may also be used to determine the quality of the voltage clamp achieved. If the reversal potential (equilibrium potential) is known, as is the case when isolation solutions limit ionic movements to only one ion, or when it is clearly established, as in the case of GABA_A receptors, currents are mediated predominantly by one ion. Under the imposed ionic conditions, currents must reverse close to the theoretical equilibrium potential for the permeable ion. In poorly voltage-clamped cells, reversal potential is either not achieved or achieved at potentials more positive than the equilibrium potential (see Fig. 11D, below, and next subsection for further discussion).

4.5.3. Conductance-Voltage Curves

If the reversal potential is known, a conductance voltage (G - V) curve can be readily calculated by dividing current at each potential by the driving force ($V - V_{\text{rev}}$). These curves are typically sigmoidal and can be fitted by a multistage Boltzmann function. Provided that current through a single channel is linear, conductance is proportional to the number of open channels. Thus, the G - V curve resembles an activation curve.

4.5.4. Steady-State Inactivation Curves

The voltage dependence of current inactivation allows one to determine the fraction of channels available for activation as a function of voltage. Currents are activated by a voltage step to potentials at which the largest conductance is achieved. This voltage step is preceded by variable prepulse potentials at which the membrane is maintained for 200 to 1,000 ms (Fig. 9A). Current amplitudes at each potential are normalized to the largest current recorded and plotted as a function of prepulse potential (Fig. 9B). These curves can be fitted to a multistage Boltzmann function. In the experiment illustrated, a potential of $\sim -80\text{ mV}$ yielded about 50% of Na_+ channels available for activation (dashed line).

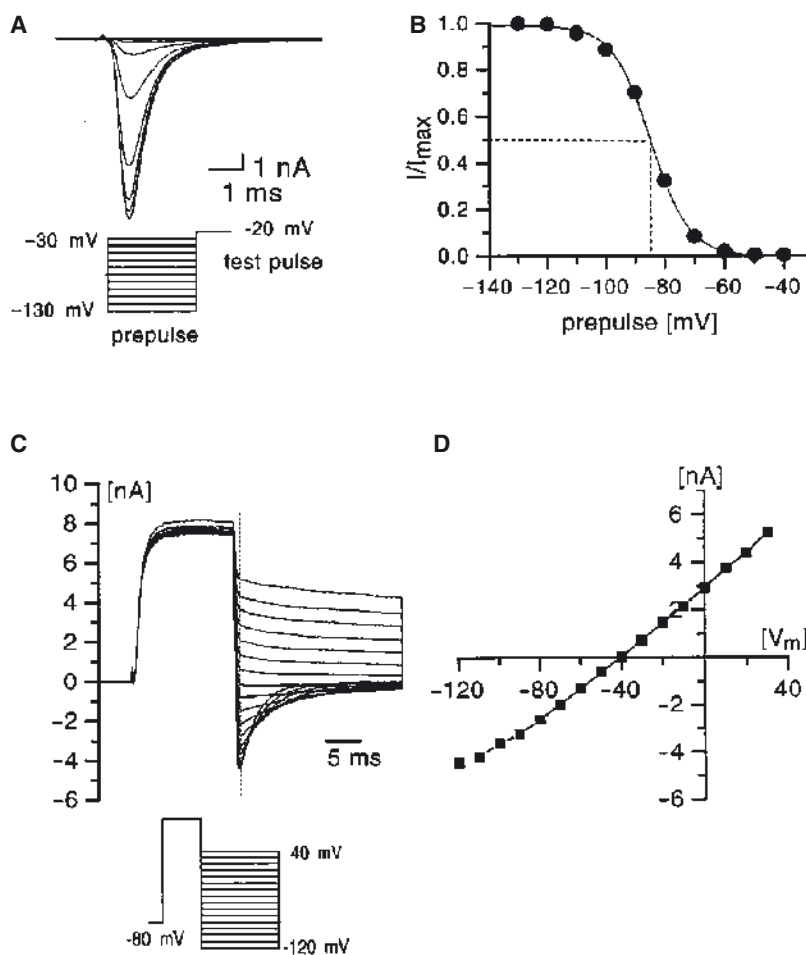


Fig. 9. Steady-state inactivation and tail-current analysis. Current recordings from two different spinal cord astrocytes. (A) To study steady-state current inactivation, inward Na^+ currents were activated by stepping the membrane to -20 mV for 8 ms. Voltage step was preceded by varying prepulse potential ranging from -130 mV to -30 mV. (B) Peak current amplitudes in A were normalized to the largest current amplitude and plotted as a function of prepulse potential. The data were fitted to a two-stage Boltzmann equation (solid line) to yield steady-state inactivation curve. (C) Tail current analysis. Outward currents were activated by a 15-ms voltage step from -80 mV to 80 mV. This step was followed by a second step to varying test potentials ranging from -30 mV to -120 mV, resulting in "tail" currents. (D) Current amplitude of tail currents was measured $500 \mu\text{s}$ after stepping potential to second step potential (dotted line) and plotted as a function of applied potential to yield tail current I - V curve.

4.5.5. Deactivation I-V Curves

As voltage-dependent currents are often also time-dependent, and may activate and/or inactivate in a time-dependent manner, *I-V* curves as described above cannot distinguish between time and voltage dependence. An elegant way to determine conductance independent of its time dependence is by analyzing the deactivation process (Fig. 9C,D). Upon termination of the voltage step, deactivation, which is the reversal of activation, results in tail currents (Fig. 9C, dotted line). Immediately after terminating the voltage step, for a brief period of time current continues to flow through open channels and only subsequently terminates with time-dependent channel closure (relaxation of tail currents). Thus, current amplitudes measured at the peak of these tails resemble time-independent current amplitudes, and these typically yield linear *I-V* curves (Fig. 9D).

4.5.6. Fitting of Time Constants

Current activation and inactivation kinetics have been well described by mathematical models. If the model is known, the data can be fitted to the model and will allow the derivation of important kinetic properties, such as time constants for activation (τ_m) and inactivation (τ_h), respectively (Hodgkin and Huxley, 1952). Often the models used are an oversimplification of the true biology. This is particularly true for fitting of whole-cell data for two reasons: (1) whole-cell current may be mediated by the combined activation of numerous channels types; and (2) even if one can be reasonably sure that currents are mediated by a single-channel population, the biophysics of this channel type, for example, the number of open and closed states, may be unknown.

Fitting routines are an integral part of numerous data acquisition or data analysis packages. Most commonly these use either a simplex or a Levenberg-Marquard algorithm to minimize the least squared error. Both algorithms are capable of producing excellent and fast fitting curves to small data sets. Examples of Levenberg-Marquard fits are demonstrated for two examples in Fig. 10. These were obtained using the script interpreter Origin (Origin Lab, Northampton, MA) by fitting to user-defined functions. The examples illustrated fitted multiple parameters simultaneously. Thus, in Fig. 10A, transient K^+ current activation and inactivation was fitted to a model of the form $f(t) = A_0 + A_1 * (1 - \exp(-(t - t_0)/\tau_m))^4 *$

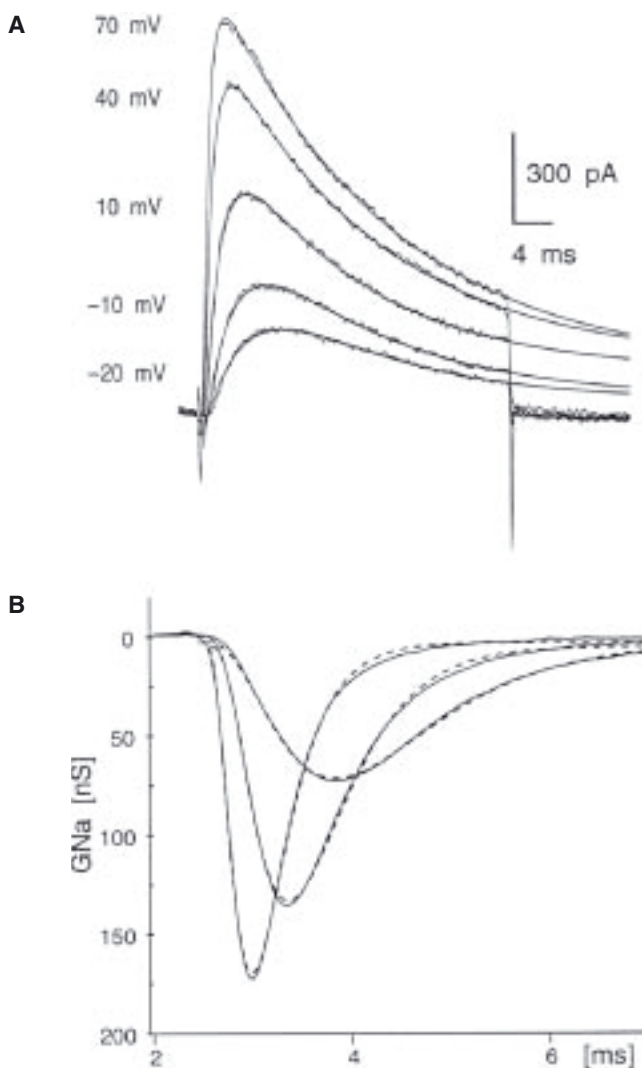


Fig. 10. Fitting of current traces using least squared fit. Transient outward K^+ (A) and inward Na^+ (B) currents were fitted to established kinetic models using a Levenberg-Marquard algorithm to minimize the least squared error. Fitted curves were superimposed on data. The models used were (A) current according to Connor and Stevens (1971) (see equation in text) and (B) the Hodgkin-Huxley (1952) equation to described Na^+ current kinetics (see equation in text). G_{Na} , sodium conductance; [nS], nano seimens.

($\exp(-(t - t_o)/\tau_h)$) as used by Connor and Stevens (1971) to describe kinetics of A currents. In Fig. 10B, Na^+ current activation and inactivation was fitted to the Hodgkin-Huxley equation: $f(t) = A_o + A_1 * (1 - \exp(-(t - t_o)/\tau_m))^4 * (\exp(-(t - t_o)/\tau_h))$ (A_o and A_1 = amplitude factors; t_o = time offset factors; τ_m and τ_h = activation and inactivation curves). It is important to keep in mind that data fits are not sufficient to formulate a model, but rather assume that the model is known and used to derive variables such as τ_m and τ_h contained in the model.

4.5.7. Data Presentation

Digitized data can be easily exported in American Standard Code for Information Interchange (ASCII) format and read into numerous powerful spreadsheet programs (Excel, Lotus, Quattro, SigmaPlot, Origin, PlotIt). There are now programs available that enable access to data without prior conversion. These programs allow electrophysiology data files to be imported for plotting, data analysis, and graphing. The authors' laboratory currently uses Origin, which is based on a scientific scripting language, LabTalk, for which a script interpreter is part of the program. This allows simple programming of frequently used commands or sequences of commands into macros, which can be assigned to visual buttons on the screen. This allows the computer-literate (nonprogrammer) to design custom data analysis and graphing schemes. As most of the graphing programs are Windows-based, merging of graphs into word processors or other drawing programs is as simple as cutting and pasting.

5. Limitations, Pitfalls, and Errors

5.1. Series Resistance and its Consequences

As mentioned previously, the major limitation of the whole-cell patch-clamp recording technique lies in its design as a continuous single-electrode voltage clamp. The continuous use of one electrode for current passage as well as voltage sensor makes true membrane voltage determination impossible. The technique assumes that pipette voltage equals membrane voltage, as voltage commands are imposed on the pipette, not on the cell. However, recording pipette and access resistance (due to potential clogging at the electrode tip) are in series with the current recording and the voltage command. This series resistor in conjunction with

the membrane resistance acts as voltage divider to all imposed voltages. Consequently, only in cases where the membrane resistance greatly exceeds the series resistance is an adequate voltage clamp (point clamp) assured. Under experimental circumstances, series resistance accounts for at least $5\text{ M}\Omega$, and more typically 10 to $15\text{ M}\Omega$. To keep the voltage error below 1%, membrane resistance has to be two orders larger than the series resistance, in our example $\sim 1\text{ G}\Omega$. This is hardly the case, and certainly does not hold true during activation of ionic currents! To ensure the best possible recording conditions, the following steps are absolutely necessary:

1. Electrode resistance has to be minimized as much as possible, depending on the size of the cells to be studied. In our experience, and dependent on the solutions used, cells from 8 to $40\text{ }\mu\text{m}$ in size can be successfully patched with electrodes in the 1.5- to $3\text{-M}\Omega$ range. However, once the whole-cell recording configuration has been achieved, it is important to frequently check for adequate compensation. If all compensation mechanisms are turned off, one may see a dramatic decrease in the magnitude of initial capacitance transients observed. The most likely explanation for such a change is the clogging of the electrode tip with cell membrane, which directly interferes with clear access to the cell's interior. This phenomenon of membrane healing around the electrode tip can be prevented by buffering $[\text{Ca}^{2+}]_i$ using high concentrations of ethylene glycol tetracetic acid (EGTA) or 1,2-bis(o-aminophenoxy) ethane- N,N,N',N' -tetra acidic acid (BAPTA). In an acute situation, slight positive or negative pressure can reverse electrode clogging. In our experience, it is possible to achieve access resistances of $5\text{ M}\Omega$ prior to series resistance compensation.
2. Series resistance (R_s) needs to be compensated for. Most patch-clamp amplifiers provide a positive feedback series resistance compensation circuit, in which a signal proportional to the measured current is added to the command potential. R_s is determined by adjusting R_s and C_p controls to square out a command voltage. Subsequently, R_s compensation is activated. Although theoretically near 100% compensation is possible, real experiments hardly allow gain setting of more than 50% to 80%. R_s compensation scales the command input to account for the voltage loss across R_s . R_s compensation is very sensitive to changes in the fast (pipette) capacitance compensation. It is

essential to adjust this compensation properly to achieve maximum percent compensation settings. Note that continuous bath perfusion may result in some oscillations of the bath fluid level. As a consequence, this would also change the effective capacitance of the pipette and would make the fast capacitance compensation unstable and thereby R_s compensation prone to ringing. Effective compensation under those circumstances thus requires a stable bath perfusion level. The problem can be reduced by the use of heavily Sylgarded electrodes, which have a much reduced capacitance.

In an ideal case, with an R_s of $10\text{ M}\Omega$, a voltage step of 100 mV results in a current flow of 1 nA , and an apparent input resistance $R_{\text{cell}} + R_s$ of $100\text{ M}\Omega$. A 1-nA current flow across R_s generates a 10-mV voltage drop across R_s and thus a 10% error. Using R_s compensation, assuming an 80% compensation, the error is reduced to 2 mV or 2% of command voltage, a tolerable error. The errors for uncompensated R_s become larger as current amplitude increases. For example, suppose activation of voltage-dependent channels gives rise to a 10 nA current, with an uncompensated R_s of $10\text{ M}\Omega$. This results in a 100-mV steady-state voltage error. Even with compensation dialed in at 80% , this still results in a 20 mV error!

3. Cells with low input resistances are almost impossible to record from. Should the membrane impedance be $<100\text{ M}\Omega$ it is advisable to increase it by inclusion of ion channel blockers to block conductances that are not of immediate interest. Thus, K^+ channel blockers could be included and Cl^- replaced by acetate to allow resolution of small Na^+ currents.

Uncompensated R_s has two additional detrimental effects on current recordings. It affects the time response to a voltage change, and it results in increased signal noise. The transmembrane voltage resulting from a step change in voltage is described by $V_m = V_c [1 - \exp(-\tau/(R_s * C_m))]$ with an effective time constant of $\tau = RC$ (if $R_s \ll R_m$). Assuming an uncompensated R_s of $10\text{ M}\Omega$ and C_m of 100 pF , charging of the membrane will be slowed with an effective time constant (τ) of 1 ms . Unfortunately, R_s will also filter any current flow recorded with this arrangement. In the absence of compensation, this results in a single pole RC filter with a -3 dB frequency described by $F = 1/(2\pi * R_s * C_m)$, resulting in a cutoff frequency (F) of 159 Hz for the above example.

5.2. Voltage-Clamp Errors

The voltage clamp is prone to error, as it makes numerous assumptions that may not be valid under the given experimental conditions. It assumes that the cell is equipotential and that the voltage measured at any one point across the membrane is the true membrane voltage. Analogously, current injection, which imposes change to the membrane voltage, is thought to be uniformly realized in all parts of the membrane, including distant processes. This, however, is not the case. As a result, two sources of error exist, namely, voltage (point) and space-clamp errors. As illustrated below, whole-cell patch-clamp recordings are even more susceptible to error than classical two-electrode recordings, and as such, the experimenter needs to be constantly aware of possible sources of this error.

5.2.1. Space Clamp

Space-clamp limitations are intrinsic to voltage-clamp and do not differ in their principles between different voltage-clamp techniques. Current injected into the cell to maintain or establish a change in membrane voltage spreads radially from the injection site and decays across distance with the space (length) constant (λ). In small-diameter spherical cells, this is a minimal concern. However, in a process-bearing cell, the current signal may have been distorted by the time it reaches distant processes hundreds of micrometers away from the injection site. In the best of circumstances, the signal will be attenuated and the voltage-changes imposed will be smaller. In the worst case, distant membranes may not experience any voltage change at all.

Double-electrode voltage-clamp methods are somewhat advantageous in that they facilitate detecting space-clamp problems more readily. In this case, the voltage electrode can be inserted at a distance from the current electrode, and closer to the site of interest. Whole-cell recordings clamp the voltage of the electrode tip, and thus provide no means to establish any true recording at a site distant from the electrode. Some investigators have chosen to insert a second patch-clamp or sharp microelectrode into cells to monitor the true voltage changes observed. Space-clamp problems can only be reduced by recording from small cells with simple morphology, ideally spherical cells. Nonspherical cells can sometimes be rounded up by exposure to trypsin or treatment with dibutylr

cyclic adenosine monophosphate (dBcAMP). However, often the most interesting cells bear extensive arborized processes. A second way to ensure that injected current can travel further is to increase the cell's impedance. Thus, it is often possible to block parts of the cell's conductance (e.g., K^+ conductance) pharmacologically to effectively increase the length constant (λ) of the cell.

5.2.2. Voltage (Point) Clamp

The whole-cell recordings technique effectively voltage-clamps the electrode tip, and, by assuming that its resistance is small relative to the cell's resistance, the cell's voltage is assumed to be clamped. As described above, this is only the case if series resistance is small and well compensated for. Unlike space-clamp errors, point-clamp errors can be readily detected and often eliminated. After canceling series resistance error (at least partially, see above) the experimenter can calculate the voltage error, which now is a linear function of current flow. Point-clamp errors produce primarily two distortions to the recorded signal: (1) slowing of current kinetics and (2) apparent attenuation of true current amplitudes due to uncompensated voltage error. Errors due to slow activation can be readily identified from the current traces.

5.2.3. Determining Quality of Clamp from I-V Plots

The *I-V* plots are a very sensitive way to evaluate point-clamp errors. Figure 11 demonstrates Na^+ current recordings from three different cells of a neuronal cell line (BIO4). Current recordings were obtained under appropriate and poor voltage control, and peak current values were plotted as a function of membrane potential and superimposed in Fig. 11D. Under the imposed ionic gradients of the recordings, the theoretical equilibrium potential for Na^+ was ~ 40 mV. The current traces in Fig. 11A yield an *I-V* plot that reverses close to sodium reversal potential (E_{Na}), indicative of proper voltage-control, whereas the traces in Fig. 11B indicate a 20-mV more positive reversal potential, and in Fig. 11C the currents do not reverse at all. Thus the *I-V* plot directly indicates the severity of the voltage errors in Fig. 11B,C. While the recording in Fig. 11B still yielded the same peak in the *I-V* relationship (at -20 mV) as the recording in Fig. 11A, the voltage step to -40 mV (arrows in

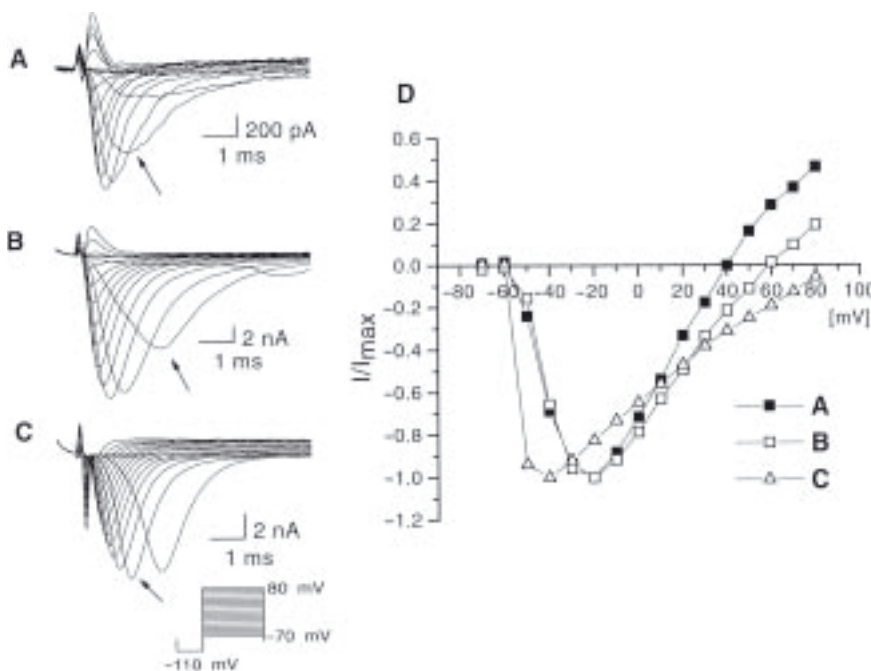


Fig. 11. *I-V* curves used to judge quality of point-clamp. (A–C) Families of current recordings from three different B104 cells (neuronal cell line) using the same step protocol indicated in inset. Peak Na^+ currents at each potential were plotted in D. Arrows in A–C point to current trace in response to a -40 mV voltage step. Only the recording in A is under appropriate point clamp. B and C are distorted by a delay in current activation at threshold (arrows) and by a shift in the *I-V* relationship (D), overestimating the true current reversal potential. E_{Na} was 40 mV .

Fig. 11A–C) was significantly delayed. In Fig. 11C, voltage control is lost at the threshold of current activation (-50 mV), and currents do not activate in a graded fashion but rather “escape” to reach near-peak amplitude with a severe delay. Similar *I-V* plots of transmitter-induced currents for which the major ion carrying the response is known (such as GABA) facilitate utilizing the reversal potential as an indicator for proper voltage control.

We have found that by minimizing R_s and utilizing *I-V* curves, currents of up to 10 nA can be properly voltage-clamped over a wide voltage range. However, under all these circumstances, poten-

tial space-clamp errors remain, and most likely currents activated in remote processes are not recorded at all.

6. Special Applications

A number of specialized applications utilize the whole-cell patch-clamp recording technique. Three of these, namely perforated patch, patch-slice, and single-cell polymerase chain reaction (PCR), are described in detailed in other chapters of this book. One application worth mentioning is the use of patch-electrodes for dye loading. As whole-cell recordings allow low resistance access to the cell's cytoplasm, it provides a convenient means to load cells with biological markers such as fluorescence indicators, horseradish peroxidase, or biotin. Loading of cells can be used to address a number of questions:

1. As fluorescence markers may diffuse through gap junctions, dye diffusion can be used to search for the existence of gap junctions between cells. Numerous fluorescent low-molecular-weight compounds that are aldehyde-fixable can be utilized for this purpose. Lucifer yellow (LY, excitation 425 nm) has been a long-time favorite. However, Invitrogen (Carlsbad, CA), offers fluorescent hydrazide salts that are available at the most commonly used wavelengths for mercury-arc lamps and lasers. Like Lucifer yellow, these dyes are fixable. The inclusion of these fluorescent fixable dyes in the patch pipette solution allows visualization during recording, assuming a fluorescent light source is available. These dyes may also be used as a cell marker, allowing the localization of a cell from which recordings were obtained. After fixation, cell-specific antibodies can be utilized to antigenically identify the cell. Alternatively, some investigators prefer the inclusion of biocytin (~0.2–0.5%) in their patch pipette solutions.
2. Although membrane-permeable acetoxymethyl (AM) esters exist for most ratiometric fluorescent indicator dyes, their characteristics can differ depending on the method of cell loading (Almers and Neher, 1985). Dyes can be readily loaded through a patch pipette through which electrophysiological recordings can be obtained simultaneously while imaging an ion of interest ratiometrically.

7. Conclusion

What started out as a spinoff from single-channel patch recordings has resulted in a technique more useful than its inventors had anticipated (Sigworth, 1986). Its ease of use makes whole-cell recordings the most widely used intracellular recording technique to date; in many instances it has replaced sharp microelectrode recordings. However, whole-cell patch-clamp recordings are notoriously prone to error and may not always generate accurate recordings. It is thus important to understand the limitations of the technique. If proper care is taken, a whole-cell patch clamp allows the study of almost any small cell of interest, and has opened the field of single-cell electrophysiology. Modifications (perforated patch) and applications of the technique to more intact preparations (patch-slice) have provided invaluable insight into nervous system function.

Acknowledgments

During preparation of this manuscript, the first author was supported by grants RO1-NS31234 and RO1-NS36692 from the National Institutes of Health.

References

- Almers, W. and Neher, E. (1985) The Ca signal from fura-2 loaded mast cells depends strongly on the method of dye-loading. *FEBS Lett.* **192**, 13–18.
- Bezanilla, F. and Armstrong, C. M. (1977) Inactivation of the sodium channel: I. Sodium current experiments. *J. Gen. Physiol.* **70**, 549–566.
- Connor, J. A. and Stevens, C. F. (1971) Voltage clamp studies of a transient outward membrane current in gastropod neural somata. *J. Physiol.* **213**, 21–30.
- Hamill, O. P., Marty, A., Neher, E., Sakmann, B., and Sigworth, F. J. (1981) Improved patch-clamp techniques for high-resolution current recording from cells and cell-free membrane patches. *Pflügers Arch.* **391**, 85–100.
- Hodgkin, A. L. and Huxley, A. F. (1952) A quantitative description of membrane current and its application to conduction and excitation in nerve. *J. Physiol. (Lond.)* **117**, 500–544.
- Hodgkin, A. L., Huxley, A. F., and Katz, B. (1952) Measurement of current-voltage relations in the membrane of the giant axon of loligo. *J. Physiol. (Lond.)* **116**, 424–448.
- Neher, E. (1982) Unit conductance studies in biological membranes. *Tech. Cell Physiol.* **P121**, 1–16.

- Neher, E., Marty, A. (1982) Discrete changes of cell membrane capacitance observed under conditions of enhanced secretion in bovine adrenal chromaffin cells. *Proc. Natl. Acad. Sci.* **79**, 6712–6716.
- Pusch, M. and Neher, E. (1988) Rates of diffusional exchange between small cells and a measuring patch pipette. *Pflügers Arch.* **411**, 204–211.
- Sigworth, F. J. (1983) Electronic design of the patch clamp, in *Single-Channel Recording* (Sakmann, B. and Neher, E., eds.), Plenum Press, New York, London, pp. 3–35.
- Sigworth, F. J. (1986) The patch clamp is more useful than anyone had expected. [Review]. *Fed. Proc.* **45**, 2673–2677.

Recommended Readings

For a more in-depth description of the patch-clamp technique, the following publications are highly recommended:

- Ferreira, H. G. and Marshall, M. W. (eds.) (1985) *The Biophysical Basis of Excitability*. Cambridge University Press, London.
- Hille, B. (2001) *Ionic Channels of Excitable Membranes*, 3rd ed. Sinauer, Sunderland, MA.
- Jones, S. (1990) Whole-cell and microelectrode voltage clamp, in *Neuromethods*, vol 14 (Boulton, A. A., Barker, G. B., and Vanderwolf, C. H., eds.), Humana Press, Clifton, NJ.
- Rudy, B. and Iverson, L. E. (1992) Ion channels, in *Methods in Enzymology* (Rudy, B. and Iverson, L. E., eds.), Academic Press, San Diego (1992).
- Sakmann, B. and Neher, E. (1995) *Single-Channel Recording*, 2nd ed., Plenum Press, New York.
- Sherman-Gold, R. (ed.) (1993) *The Axon Guide for Electrophysiology and Biophysics Laboratory Techniques*, Axon Instruments, Inc., Sunnyvale, CA.

Patch-Clamp Analysis

Advanced Techniques

Walz, W. (Ed.)

2007, X, 475 p. 97 illus., Hardcover

ISBN: 978-1-58829-705-1

A product of Humana Press